MEASUREMENT OF MARKSTEIN LENGTHS IN LAMINAR SPHERICAL EXPLOSION FLAMES

E. M. J. Mushi
Department of Mechanical Engineering
University of Dar es salaam
P. O. Box 35131 Dar es salaam

Abstract

Schlieren photography was used to record the development of spherical flames in a combustion bomb. Flame speed and flame stretch were evaluated from the data and used to evaluate Markstein lengths and numbers. The results indicate a strong influence of both the spark discharge energy and equivalence ratio. Low spark discharge energy is observed to give rise to more unstable flames compared to high energy sparks. It is observed that for the range of energy tested, 80 and 400 mJ gave the best stability for the flames. For equivalence ratio less or equal to 1.225 an 80 mJ discharge results in flames which are less susceptible to instabilities. The relationship between equivalence ratio and both Markstein number and length can be accurately represented by a third order polynomials for spark discharge energy of 500 mJ.

Introduction

The Markstein length, *L*, characterizes the stability of a flame and also the influence of flame stretch upon the burning rate. When normalized by the laminar flame thickness, δ_l, it gives the Markstein number, Ma, which together with the Karlovitch stretch factor, K, quantify the effect of flame stretch upon the turbulent burning velocity. Though the Markstein length can be computed, its accurate experimental evaluation is of vital importance in that the results can be used to corroborate its mathematical evaluation. Measurements can be done in two ways, one being through observation of flame instability [1]. The other method utilizes the flame speed of spherically expanding laminar flames at constant pressure [2]. The second method is preferred in this work because laminar spherical propagation is well defined for unambiguous measurement of flame speed [3].

Considering a flame surface area A, which increases by, dA, within a time interval, dt, the flame stretch, α is given by eq. 1

$$\alpha = dA/Adt \qquad (1)$$

For small values of flame stretch, the difference between the unstretched and stretched burning velocity is equal to the product of the flame stretch and the Markstein length, eq. 2.

$$u_l - u_n = \alpha L \qquad (2)$$

Following a similar argument the unstretched laminar flame speed, S_l, and the stretched flame speed, S_n, are related by eq. 3 where L_b is the burned gas Markstein length.

$$S_l - S_n = \alpha L_b \qquad (3)$$

The finite thickness of the flame and uncertainties as to the position of where the flame stretch should be defined do pose a problem in the measurements. The surface to be used must be the one which defines the propagation speed. In this work this surface is defined as the boundary for the stationary burned gas behind the flame. The measurements, schlieren technique used in this work and others, define a propagating front which is ahead of the stationary burned gas surface. Little is known of the distance of separation between the two surfaces. If we assign a value of, Δ, to this separation then eq. 3 can be rewritten in terms of the schlieren radius, r, and Δ, eq. 4

$$S_l - \frac{d(r-\Delta)}{dt} = \frac{2}{(r-\Delta)}\frac{d(r-\Delta)}{dt}L_b \qquad (4)$$

Assuming the magnitude of $d\Delta/dt$ to be negligibly small compared to dr/dt and further

Published by the Faculty of Engineering University of Dar es salaam
P. O, Box 35131, Dar es slaam, Tanzania

that Δ can be neglected in comparison to r then eq. 5 is obtained, where S_c = dr/dt, the speed of the schlieren front and α_c=(2dr/dt)r^{-1} is the flame stretch associated with the schlieren front surface.

$$S_l - S_c = \alpha_c L_b \qquad (5)$$

As the spherical flame develops, it tends to change towards a planar flame as the radius increases. This implies that for a laminar flame the stretch associated with the schlieren surface will tend towards zero. It follows from this that if the speed of the schlieren surface is plotted against the stretch associated with the same surface, the value of the schlieren surface speed at zero stretch will give the value of the unstretched flame speed, S_s. The gradient of the curve as it approaches zero stretch, will give the value of the burned gas Markstein length, L_b. The unburnt gas Markstein number can be evaluated from the burned gas length using eq. 6 [4]

$$L - \frac{\rho_b}{\rho_u} L_b = \delta_l \ln\left(\frac{\rho_u}{\rho_b}\right) \qquad (6)$$

The laminar flame thickness is evaluated as the ratio of the kinematic viscosity of the cold mixture to the laminar burning velocity ($\delta_l = v/u_l$).

Experiments

The experiments described in this work were conducted in a fan-stirred explosion bomb. This comprised a cylinder of 305mm diameter and 305 mm length with a 150mm diameter concentric window on each end plate. These windows provided optical access for schlieren photography of explosion flames.

Flame propagation was recorded by a high speed cine' camera using the schlieren technique. This employed a Spectra-Physics 10 mW helium-neon laser, model 106-1, with a beam diameter of 0.65 mm and wavelength of 632.8 nm. The laser beam was first passed through an Olympus A40 microscope objective lens placed at the focal point of a 150 mm diameter lens with 1000 mm focal length. A 1 mm diameter pin hole was placed close to the microscope objective. This arrangement produced a 150 mm diameter parallel beam which passed through the bomb windows. From the bomb the parallel beam passed through another 150 mm diameter lens with a focal length of 500 mm, which focused the beam on a 0.65 mm pinhole placed 500 mm from the lens. Attached to the pinhole was a bandpass filter to pass only the He-neon laser radiation. Behind the 0.65 pinhole was a Hitachi high speed camera, model 16HM, with a 35 mm lens run at a speed of 5000 frames per second. This recorded the schlieren images of the flame on an Ilford FP4 16 mm high speed film.

A variable discharge duration ignition system was used for the ignition of the combustible mixture in the bomb. A breakdown unit consisting mainly of a car ignition coil which was energized such that it total energy was just enough to provide breakdown of the spark gap at an electron gap of 0.6 mm without causing ignition of a combustible mixture was used. The breakdown was achieved by providing a one microsecond 300 V pulse into the primary coil of the ignition coil. The secondary coil was connected to the spark plug via a 400 kΩ, high voltage resistor and a high voltage diode which was only forward biased when the secondary coil voltage was high

The main spark was achieved using the discharge of a 40 μF capacitor through the spark gap via a bank of resistors which controlled the discharge current. This capacitor was charged using a 600 V D.C supply. A timing unit was used to short the capacitor and thus end the discharge. The voltage drop across a 4.7 Ω low induction resistor in series with the spark gap, was used to evaluate the spark current. The voltage drop across the spark gap was measured directly. Oscilloscope traces of the variation of both this voltages during the discharge were photographed using polaroid camera and further digitised and processed to give a history of the gap voltage and current over the discharge period. Numerical integration of the product of the gap voltage drop and the current, over the discharge duration provided the total energy discharged.

Two identical electrodes were mounted opposite to each other in the cylindrical walls of the combustion vessel such that they met at the centre, where a gap of 0.6 mm was maintained.
Two metal markers attached to the bomb window, 60 mm apart, provided a scale for the recorded images. Their images were simultaneously recorded on the film with the schlieren image of the flame. Lengths measured on the projected images from the processed film were converted to actual lengths in the explosion using the marker calibration.

The developed films were projected one frame at a time on a Panasonic Telecine adapter, model WV-J20AE, which was coupled to a Panasonic CCD camera, model WV-BL600, using a wide angle 28 mm lens. This image was further read from the camera by a Nec PowerMate 386/20.

The outer edge of the digitized flame image was manually traced using a mouse. The resulting data representing the coordinates of the discrete points along the edge were numerically integrated to give the projected flame area.

The radius of the circle with an enclosed area equal to the projected flame area was found and this was taken as the equivalent flame radius for the frame. The frame time was established using a timing mechanism built into the high-speed camera. This consisted of a light emitting diode, (LED), flashing at 1kHz to produce a timing mark on the film at intervals of one ms.
Another important facility on the high-speed camera was an event marker, which was another LED set to produce a mark on the film at the start of an event. This was set to mark the film at the beginning of the spark discharge. Combined use of these markers gave the necessary information to establish the time corresponding to a given frame, from the start of the spark discharge. From this a radius versus time plot traced the history of the explosion.

Flame speed data were obtained from the radius-time data using numerical differentiation. The accuracy of this numerical technique depends on the interpolation method and hence different methods were tried and compared graphically. Cubic spline interpolation was found to produce the best fit for the data and therefore was used. The schlieren surface stretch was obtained by dividing the schlieren surface speed by half the associated schlieren radius.

The condition that $\alpha_c=0$ will require a very large bomb for constant pressure explosions. The explosion bomb used had a limited volume for constant pressure explosions but gave a clear indication of the change towards the plane flame. The results from the limited explosions were extrapolated to a condition which will correspond to $\alpha_c=0$.

Five explosions were conducted for each condition and the results averaged. This does smooth the data to a certain extent and improves accuracy.

Results and discussion

Figure 1 shows a typical variation of schlieren surface speed and corresponding stretch against schlieren radius. It shows that the period during the discharge and shortly after is associated with the decay of discharge enhanced propagation. This explains the decreasing high speed and stretch to a minimum before increasing. The following increase is associated with increase in the chemical reactions. This increase is observed to decrease with increase in the size of the flame. While the flame speed continues to increase with diminishing rate, the stretch quickly attains a maximum value and starts to decrease as the flame grows. This is in agreement with the theory that a spherical flame will tend to behave as a plane flame as it develops.

Figure 2 gives a typical variation of flame speed with flame stretch at an equivalence ratio of 1.25 for two different spark discharge durations. Initially the spark which ignites the mixture result in high values of stretch which decreases with time. It follows from this that the respective curves are traced from left to right. Ignition is represented by the right end of the curves. As the flame develops the influence of the spark decreases and hence the associated flame stretch. This implies following the curves from right to left. On reaching the minimum stretch the influence of the spark becomes minimal while chemical reactions in the flame start to increase thus initiating an increase in the stretch. Under these conditions both the stretch and the flame speed do increase. However the increase in flame stretch with flame speed decreases with flame speed to a minimum. flame stretch. This is followed by one in which the flame speed increases slowly as the flame stretch decreases. The work presented in this paper is focused in this region where it is assumed that the behavior of the flame is approximately that of a planar one. It is also evident from this figure that the energy released by the spark does play an important role in changing the value of the associated flame stretch. Despite indicating similar behavior, the lower energy spark is seen to give slightly lower flame stretch compared to the 500 mJ spark .Figure 3 shows the influence of spark discharge energy on Markstein lengths and numbers. These show similar behavior against spark discharge energy. They are observed to increase with spark energy from 80 mJ to a local maxima which occurs at approximately 200 mJ. This is followed by a decrease to a local minima which occurs at 400 mJ except for the burned gas Markstein number which attains a minima at around 450 mJ. Beyond this local minima there is an increase in the respective lengths and numbers with discharge energy. The curves shown on the figure are third order least square polynomials fitted to the experimental data. It is evident from Fig. 3 that there is significant influence of the spark discharge energy on the behavior of the flame. For improved behavior with good flame stability both Markstein length and number have to be low. It follows from this that the best condition is that with minimum values of all the above parameters. In this context 83 and 400 mJ discharges are the best for the conditions understand. This observation is significant in that not always high energy discharge will ensure better flame propagation and stability.

Beyond the minimum stretch, flame speed increases without appreciable change on the flame stretch. This is followed by one in which the flame speed increases slowly as the flame stretch decreases. The work presented in this paper is focused in this region where it is assumed that the behavior of the flame is approximately that of a planar one. It is also evident from this figure that the energy released by the spark does play an important role in changing the value of the associated flame stretch. Despite indicating similar behavior, the lower energy spark is seen to give slightly lower flame stretch compared to the 500 mJ spark.

Figure 3 shows the influence of spark discharge energy on Markstein lengths and numbers. These show similar behavior against spark discharge energy. They are observed to increase with spark energy from 80 mJ to a local maxima which occurs at approximately 200 mJ. This is followed by a decrease to a local minima which occurs at 400 mJ except for the burned gas Markstein number which attains a minima at around 450 mJ. Beyond this local minima there is an increase in the respective lengths and numbers with discharge energy. The curves shown on the figure are third order least square polynomials fitted to the experimental data. It is evident from Fig. 3 that there is significant influence of the spark discharge energy on the behavior of the flame. For improved behavior with good flame stability both Markstein length and number have to be low. It follows from this that the best condition is that with minimum values of all the above parameters. In this context 83 and 400 mJ discharges are the best for the conditions understand. This observation is significant in that not always high energy discharge will ensure better flame propagation and stability.

The local maxima in the indicated parameters highlights conditions far from the optimum

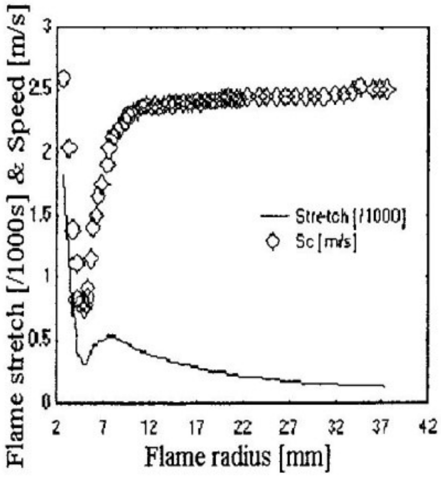

Fig. 1 Flame speed Sc vs Flame stretch

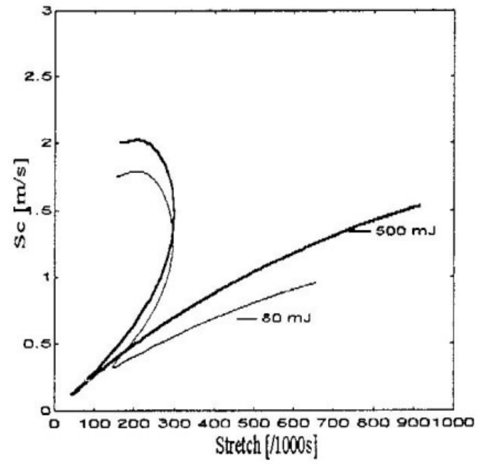

Fig. 2 Flame speed & stretch vs Flame radius

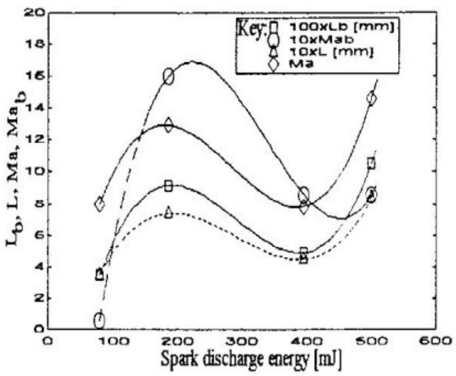

Fig. 3 Influence of spark disharge energy

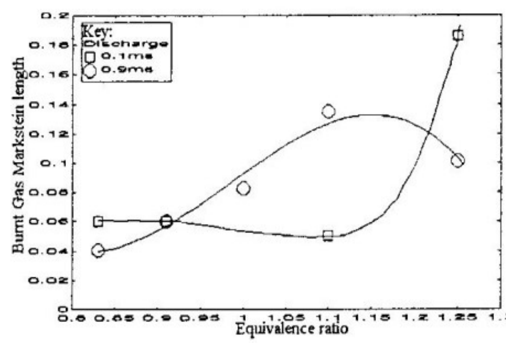

Fig. 4 Burnt gas Markstein length vs Equivalence ratio

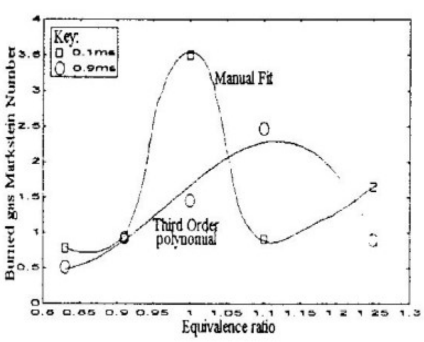

Fig. 5 Markstein length vs Equivalence ratio

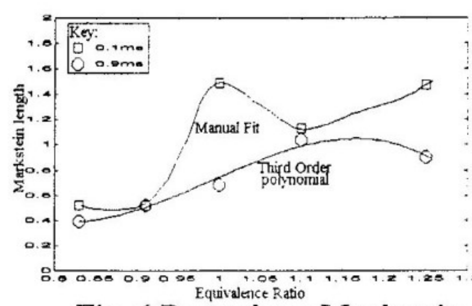

Fig. 6 Burned gas Markstein number vs Equivalence ratio

and are to be avoided for better performance. For the range of discharge energy covered there are two cases of minimum values. This is favorable in that under certain conditions the 83 mJ discharge spark may be too low for flame propagation. In this case 400 mJ can be used.

Figure 4 shows the variation of the burned gas Markstein length with equivalence ratio for two spark discharge durations, 0.1 and 0.9 ms, which correspond to 83 and 500 mJ discharge energies respectively. The 500 mJ discharge is observed to give a uniformly increasing burnt gas Markstein length from 0.063 at θ=0.83 to a maximum value of 1.056 at equivalence ratio of 1.15. The length decreases with further increase in the equivalence ratio. The solid curve gives a least square polynomial fitted to the experimental data.

The 83 mJ (0.1ms) discharge flames indicated a burned gas Markstein length which is approximately constant for equivalence ratios ranging from 0.83 to 1.1. Beyond θ=1.1 there is a significant increase in the length to a value of 0.185 mm at equivalence ratio of 1.25. The solid curve shown on the figure was manually fitted to indicate the trend. It follows from this that between equivalence ratios of 0,83 and 0.9 the 0.9 ms discharge results in more Stable flames. This is also the case for equivalence ratios higher than 1.22. Between 0.9 and 1.225, a 0.1 ms discharge results in flames which are more stable. The difference in the burned gas Markstein number for the two spark discharges at an equivalence ratio of 0.83 can be considered small and hence negligible compared to the difference at other equivalence ratios. It can be concluded from this that for equivalence ratio less or equal to 1.225 the 0.1 ms discharge is superior in establishing stable flames.

Figure 5 shows the evaluated Markstein length for the two spark discharges at different equivalence ratios. For 0.9 ms spark discharge flames the Markstein length increases with equivalence ratio to a maximum value of 1.064 at an equivalence ratio of 1.164. The length decreases with further increase in equivalence ratio beyond 1.164. Flames initiated by the 0.1 ms spark discharge indicate a different behavior in which the Markstein length decreases slightly with increase in equivalence ratio from 0.83 to 0.9 before increasing to a local maxima of 1.49 mm at 1.0. The length decreases to a value of 1.1336 mm at equivalence ratio of 1.1 before increasing again to 1.47mm at equivalence ratio of 1.25. The behavior of the 0.9 discharge flames is well represented by a third order polynomial fitted to the experimental data. Except for equivalence ratio of 1.0 where the Markstein length is observed to increase considerably the difference between the two discharges is not significant for Markstein lengths.

Figure 6 presents burnt gas Markstein number for different equivalence ratios and for flames ignited by sparks having discharge durations of 0.1 and 0.9 ms respectively. Again the trend for the 0.9ms discharge flames the trend follows that of the burnt gas Markstein length in which it increases with equivalence ratio from a

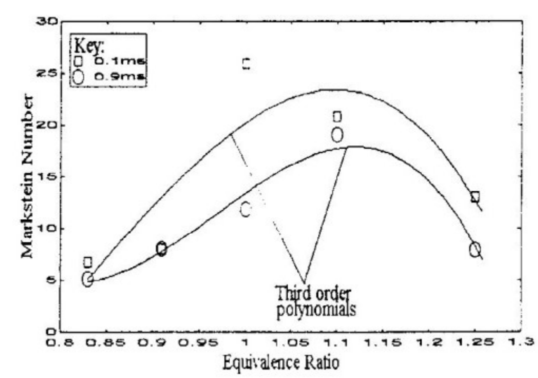

Fig. 7 Markstein Number vs Equivalence ratio

value of 0.51 at equivalence ratio of 0.83 to maximum of 2.3232 at equivalence ratio of 1.123. This length decreases for equivalence ratio greater than 1.123 to a value of 0.9119 at equivalence ratio of 1.25. The least square polynomial fit is represented by equation 13.

For flames initiated by the 0.1 ms discharge the burnt gas Markstein number is observed to increase gradually between equivalence ratios 0.83 and 0.91. This is followed by a rapid increase to a maximum value of 3.5 at equivalence ratio of 1.0. Beyond equivalence ratio of 1.0 the number decreases to a value of 0.8889 at equivalence ratio of 1.1. There after it increased to a value of 0.9119 at equivalence ratio of 1.25. The solid curve shown for the respective data was manually fitted to show the trend.

Markstein Numbers evaluated from the experimental data are presented on fig. 7 for different equivalence ratio. A least square third order polynomial fitted to the data for 0.9 ms discharge is observed to represent the experimental data well. The Markstein number increases from a value of 5.11 at equivalence ratio of 0.83 to a maximum value of 18.03 at equivalence ratio of 1.1179. This is followed by a decrease in the number for equivalence ratios higher than 1.1179 to a value of 7.96 at equivalence ration of 1.25.

For the 0.1 ms discharge flames the trend is similar to that of the burned gas Markstein number in that it increases gradually between equivalence ratios 0.83 and 0.91. This is followed by a rapid increase to a maximum value of 25.98 at equivalence ratio of 1.0. Beyond equivalence ratio of 1.0 the number decreases gradually to a value of 13.0 at equivalence ratio of 1.25. The solid curve shown for the respective data was manually fitted to show the trend.

Conclusion

There is significant influence of spark discharge energy on Markstein lengths and numbers which indicates two optimum conditions namely 80 and 400 mJ respectively. Outside this two values flames become susceptible to increased instability.

The influence of discharge energy on Markstein numbers and lengths can be approximated accurately using third order polynomial.

For equivalence ratio less or equal to 1.225 the 0.1 ms discharge results in flames which are less susceptible to instabilities.

Stoichiometric flames are observed to be more unstable compared to flame at other equivalence ratio when low spark discharge energy is employed.

Changing the discharge energy/duration does not alter significantly the behavior of the flame for equivalence ratio less than or equal 0.9.

The relationship between equivalence ratio and both Markstein lengths and numbers can be represented accurately by third order polynomials for spark discharge energy of 500 mJ.

List of Symbols

A Flame area
E Spark discharge energy
L Markstein length
Ma Markstein Number
r Flame radius
S Flame speed
t Time
u Burning velocity

Greek symbols:

Δ Separation between stationary burned gas and propagating flame front
δ Flame thickness
θ Equivalence ratio
ρ density

Subscripts

b based on burnt gas
c associated with the schlieren front
1 unstretched
n stretched

References

1. Searby, G. And Quinard, J., Combustion and Flame No. 82, 1990 pp 298

2. Dowdy, D. R., Smith, D. B. and Taylor, S. C. Twenty third Symposium (International) on Combustion, The Combustion Institute, 1991, pp 325
3. Dixon-Lewis, G., Twenty third Symposium (International) on Combustion,
4. The Combustion Institute, 1991, pp 305
5. Clavin P., Progress in Energy and Combustion Science, 11:1, (1985)